EARLY METAL-SILICATE DIFFERENTIATION AND PARENT BODY PROCESSES REVEALED FROM THE HIGHLY SIDEROPHILE ELEMENT SYSTEMATICS OF WINONA. X.J. Zhang[1], R.W. Nicklas[1,2], and J.M.D. Day[1]. [1]Scripps Institution of Oceanography, La Jolla, CA 92037, USA. [2]Boston College, Chestnut Hill, MA 02467, USA. Email: xmjzhang@ucsd.edu

Introduction: Primitive achondrites are a class of meteorites including the winonaite-IAB group, characterized by metamorphic or igneous petrological textures and near-chondritic bulk compositions [1-3]. Primitive achondrites are interpreted to be products of high degrees of metamorphism and limited partial melting of a variety of parent planetesimal bodies with broadly chondritic precursor compositions [2-5]. Therefore, primitive achondrites provide valuable records of processes involved in early stages of planetary differentiation in the Solar System [5-6].

Like other primitive achondrites, winonaites exhibit textural, mineralogical, and geochemical evidence of incomplete planetary differentiation [2-5]. For example, type specimen Winona has equigranular, recrystallized textures and abundant triple junctions [3]. Parent body heating created temperatures that reached the Fe,Ni-FeS cotectic (~950-980 °C; [7-8]) and initiated low degrees of partial melting in Winona [3], inferred from its iron-nickel metal and troilite veins [2-3] and two-pyroxene equilibration thermometry (1070 °C; [9]). Additionally, Winona may record silicate partial melting of the parent body, containing coarse-grained olivine-rich regions [3]. However, characterizing effects of early partial melting in the winonaite parent body has been challenging, not only because of pervasive terrestrial alteration [3-4], but also due to mineralogical and compositional heterogeneities [1-5] (*e.g.*, variable rare-earth element abundance patterns [4-5]) within individual winonaite samples. Consequently, the extents of metal-silicate differentiation and silicate partial melting in the winonaite parent body are debated [2-5].

Highly siderophile elements (HSE: Re, Au, Pd, Pt, Rh, Ru, Ir, Os) preferentially partition into metal and sulfide compared to silicate melts [10]. Therefore, HSE abundances and ^{187}Re-^{187}Os systematics are sensitive geochemical tools for assessing metal-silicate segregation effects and initial heterogeneities of primitive achondrite parent bodies [11]. To further constrain the partial melting processes and internal heterogeneities of the winonaite-IAB parent body, we present the first HSE abundance and Re-Os isotopic data, along with trace element abundances of bulk Winona and separates.

Samples and Methods: Around four grams of Winona was powdered by hand using an agate pestle and mortar. For bulk rock major- and trace-element analysis, two homogenized sample aliquots (20-25 mg), were dissolved with 3 mL of Teflon Distilled (TD) 29N HF and 0.75 mL of TD 15.7M HNO_3 in Parr Bomb vessels and Teflon beakers respectively. The resulting clear solutions were measured using an *iCAP Q* ICP-MS analysis at the Scripps Isotope Geochemistry Laboratory (SIGL). Reproducibility of reference geostandards was generally better than ± 4% (RSD).

Two polished thick sections (627A, 627B) of Winona were used for *in situ* electron microprobe (EPMA) and laser ablation ICP-MS analyses (LA). Major element concentrations of all phases were determined by EPMA at the University of Nevada Las Vegas, while lithophile trace element and HSE concentrations of major phases were determined by LA-ICP-MS at the SIGL. For whole rock and fraction HSE abundances and Re-Os isotope analysis, fragments of Winona 627A and 627B were roughly crushed by hand using an agate pestle and mortar. A hand magnet was used to separate metal (magnetic) and silicate (non-magnetic) fractions. A bulk powder aliquot and 12 Winona separates (including 8 magnetic) of 1 to 11 mg, were prepared with multi-element spikes (ID) and digested with inverse Aqua Regia in Carius tubes at a maximum temperature of 270 °C in an oven for three days. Abundances and isotopic compositions of Os were measured with a Thermo Scientific *Triton* thermal ionization mass spectrometer (TIMS) in negative-ion mode at the SIGL. Analytical uncertainty of ^{187}Os/^{188}Os for 35 pg UMCP standards was 3.6‰ (2SD). The remaining HSE abundances were measured by *iCAP Q* ICP-MS at SIGL, with a reproducibility better than 1% for 5 ppb solutions.

Results and Discussion: Rare earth element (REE) abundance patterns of Winona are shown in Figure 1. Results from two separate Winona aliquots digested in Parr Bomb and Teflon beaker agree well.

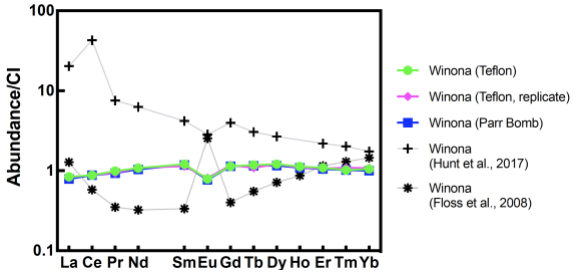

Figure 1. *Bulk rock REE abundances of Winona normalized to CI [12]. Results from this study are compared to previous whole-rock and calculated values [4-5].*

Compared to Winona REE data from [4], Winona samples in this study are not strongly affected by terrestrial alteration, as shown by their lack of a Ce anomaly and low Ba content. Winona shows a relatively flat REE pattern with slight depletions in Eu and the light REE, suggesting broadly chondritic bulk compositions and the onset of silicate partial melting due to mobilization of plagioclase-rich melts [3,5]. Compared to modal recombined REE abundances enriched in Eu, calculated by [5], Winona from this study may contain higher proportions of orthopyroxene and/or clinopyroxene, due to heterogeneity in this relatively coarse-grained, and variably terrestrially altered meteorite.

HSE abundances of whole-rock and fractions of Winona are shown in Figure 2a. Bulk Winona shows an inherently non-chondritic HSE signature with enrichment in Pd and some inter-HSE fractionation, potentially suggesting mobilization of sulfides. Metal and silicate Winona separations both exhibit variabilities in HSE abundances. Silicate fractions all show high Re/Os, with variable HSE fractionation. Some magnetic fractions have HSE abundance patterns resembling bulk Winona, while others show higher Re/Os, indicating that separations do not represent pure phases.

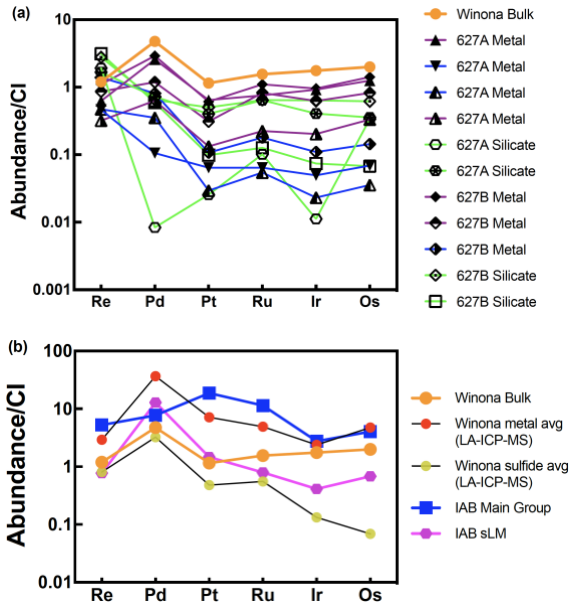

Figure 2. *Winona whole-rock and mineral fraction HSE abundances normalized to CI chondrites [11, 13-14]. (a) ID HSE abundances of bulk Winona and separates. (b) LA HSE abundances of metal and sulfide compared to IAB iron meteorites [15].*

Average HSE abundances of metals and sulfides determined by LA-ICP-MS (Fig. 2b) indicate that the Pd-rich phase of Winona is metal. HSE patterns of IAB irons determined by [15] show that Winona metal is unlike main group IAB irons, but similar to the IAB sLM subgroup, suggesting a genetic relation to them.

Rhenium-osmium isotope compositions are shown in Fig. 3. Bulk Winona has $^{187}Os/^{188}Os$ of 0.1256 ± 0.0001 (2SD), agreeing with the calculated $^{187}Os/^{188}Os$ from recombination of Winona fractions (0.1256 ± 0.0005, 2SD), suggesting a carbonaceous chondrite-like initial composition [11, 13-14] of the winonaite-IAB parent body. Winona fractions show large variations in $^{187}Os/^{188}Os$ ranging from 0.1205 to 0.1338. Silicate, recombined, and some metal-rich Winona fractions have high Re/Os potentially contributed by terrestrial weathering [3, 13-14]. Metal-rich Winona fractions with low Re/Os also exhibit $^{187}Os/^{188}Os$ variations ranging from 0.1205 to 0.1280, which may suggest initial small-scale Os heterogeneities within Winona or very early parent body processing.

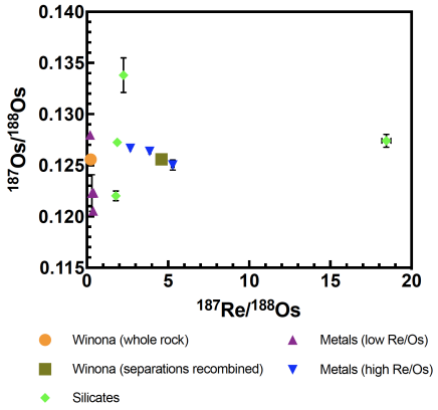

Figure 3. *The $^{187}Re/^{188}Os$ and $^{187}Os/^{188}Os$ ratios of Winona whole-rock, fractions and calculated recombination of fractions. Error bars (2SD) are typically smaller than symbols.*

Acknowledgments: We thank the MGMH for provision of speciments of Winona (M627, M55A). This work was supported by the NASA Emerging Worlds program (80NSSC19K0932).

References: [1] Prinz M. et al. (1983) *LPS XIV*, pp 616-617. [2] Benedix, G.K. et al. (2000) *Meteoritics & Planet. Sci.*, 35, 1127-1141. [3] Benedix, G.K. et al. (1998) *GCA*, 62, 2535-2553. [4] Hunt A.C. et al. (2017) *GCA*, 199, 13-30. [5] Floss C. et al. (2008) *Meteoritics & Planet. Sci.*, 43(4), 657-674. [6] Dhaliwal J.K. et al. (2017) *GCA*, 216, 115-140. [7] Kellerud G. (1963) *Ann. Rep. Geophys. Lab.* 67, 4055–4061. [8] Kubaschewski O. (1982) *Iron-Binary Phase Diagram.* Springer. [9] Bild R.W. (1977) *GCA*, 41, 1439-1456. [10] Barnes S.J. et al. (1985) *CG*, 53(3-4), 303-323. [11] Day J.M.D. et al. (2016), *Rev. Mineral. Geochem.*, 81, 161-238. [12] McDonough W.F. and Sun S.S. (1995), *CG*, 120(3-4), 223-253. [13] Horan M.F. et al. (2003), *CG*, 196, 27-42. [14] Fischer-Gödde M., (2010) *GCA.*, 74, 356-379. [15] Worsham E.A. et al. (2016) *GCA*, 188, 261-283.